ELSEVIER

Journal of Molecular Structure: THEOCHEM 732 (2005) 161–171

THEO CHEM

www.elsevier.com/locate/theochem

# Ring expansions in substituted phenylnitrenes: an AM1 SCF-MO study

Peter G.S. Dkhar, R.H. Duncan Lyngdoh*

*Department of Chemistry, North-Eastern Hill University, Shillong 793022, India*

Received 6 November 2004; accepted 2 March 2005
Available online 8 September 2005

**Abstract**

The semi-empirical AM1 SCF-MO method is used to study the ring expansion of *ortho*-substituted phenylnitrenes in the singlet state. This two-step rearrangement involves nitrene atom insertion into the phenyl ring to give a bicyclic azepine intermediate, which undergoes electrocyclic ring opening to yield the monocyclic keteneimine product. The first step of nitrene insertion in *ortho*-substituted phenylnitrenes may occur either towards the substituent side or away from it, while the second step is simply sequential to the first. Nine *ortho*-substituted phenylnitrene systems X–$C_6H_4$–N (X = H, $CH_3$, CN, $NH_2$, $NO_2$, OH, F, SH and Cl) are considered for study here.

Comparison of activation energy barriers for both steps predicts that the first step of azepine formation would be the rate-determining step. Electron-withdrawing substituents promote this step, and vice versa for electron-donating ones. The azepine intermediate is unstable compared to the keteneimine product due to strain. The transition state for the second step is predicted to have aromatic character, unlike the azepine and ketenimine. In general, the ring expansion is predicted to be favoured towards the unsubstituted side of the ring rather than towards the substituted side, where steric factors play the major role. The two successive steps of the ring expansion proceed via transition states which are more or less similar to each other, the second one having aromatic character. Competition between ring expansion and decay of the singlet phenylnitrene to the triplet state, as estimated by calculated enthalpy terms, is predicted to favour decay to the triplet state.
© 2005 Published by Elsevier B.V.

*Keywords:* Phenylnitrene ring expansion; Nitrene singlet and triplet states; AM1 SCF-MO method

## 1. Introduction

Rearrangements in singlet nitrenes have been well studied experimentally, and include 1,2 hydride and alkyl group migrations in alkyl- and acylnitrenes, leading to imine and isocyanate products [1,2]. Rearrangement can also occur in phenylnitrene in a manner similar to that in phenylcarbene [3–5], and may compete with intersystem crossing to the triplet state (which does not yield such ring expansion products). This ring-expansion rearrangement of phenylnitrenes [1,2] occurs by a reversible two-step pathway involving a bicyclic azepine intermediate and a seven-membered ring keteneimene product. Earlier theoretical studies on arylnitrene ring expansions [6–12] are summarized below. This semi-empirical AM1 SCF-MO study treats the ring expansion of nine different singlet *ortho* substituted phenylnitrenes.

### 1.1. Ring expansion mechanism

Thermolysis or photolysis of phenylazide yields the phenylnitrene, which as a singlet species can undergo ring expansion in two steps, firstly to a bicyclic azepine intermediate, which then further rearranges to a seven-membered ring keteneimine product, which may be trapped by nucleophiles [13–15]. The bicyclic structure of azepine as such has never been observed directly, unlike the monocyclic keteneimene [15–34]. However, the analogous azirine species has been characterized [35] by IR and evidence exists for its intermediacy in various reactions. This two-step mechanism for phenylnitrene rearrangement has been generally accepted as a result of numerous studies [15–34] and is also supported by various theoretical calculations [6–12]. Furthermore, the existence of the keteneimine has been confirmed by matrix [29–31,35] and solution spectroscopic studies [32]. The ring expansion reaction has been shown to involve only the singlet state of the nitrene, which therefore competes with intersystem crossing to the triplet ground state of the phenylnitrene.

* Corresponding author. Tel.: +91 2642722614; fax: +91 3642722602.
*E-mail address:* rhdl@nehu.ac.in (R.H.D. Lyngdoh).

0166-1280/$ - see front matter © 2005 Published by Elsevier B.V.
doi:10.1016/j.theochem.2005.03.005

The two successive steps of ring expansion are thus (i) nitrene insertion into the aromatic ring forming the bicyclic azepine intermediate, and (ii) electrocyclic ring opening of the azepine to give the keteneimine product, as shown in Fig. 1. In the first step, the nitrene atom inserts itself into the C═C bond next to it on the phenyl ring. The exocyclic nitrene group may insert towards either the unsubstituted or substituted sides of the ring, as shown in Fig. 1(a) and (b) respectively, so that the two possibilities can compete. The first step creates the bicyclic azepine intermediate (available in two isomeric forms due to the two paths possible for the first step). The second step follows automatically, being determined by the first, and is actually a pericyclic reaction (electrocyclic ring opening), where a C–C σ bond within the bicyclic system cleaves as the conjugated π system rearranges within the azepine, so that a seven-membered monocyclic keteneimine forms (in two isomers). The keteneimine product itself is a reactive species, and susceptible to attack by nucleophiles at the carbon adjacent to the ring nitrogen, e.g. when water adds to the keteneimine, an unsaturated ε-lactam is the product.

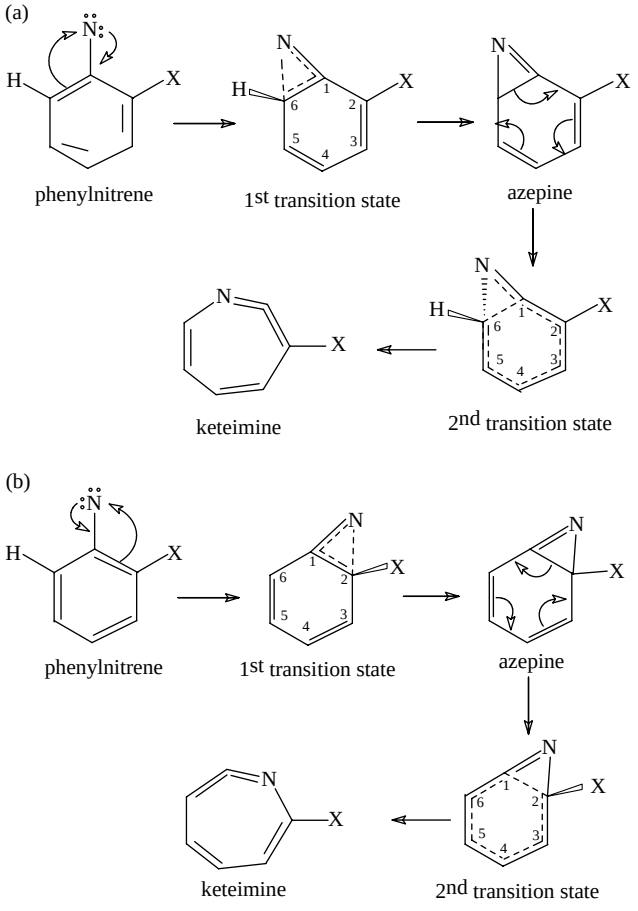


Fig. 1. Schematic diagram for the ring expansion of *ortho*-substituted phenylnitrenes towards (a) the unsubstituted side, and (b) substituted side.

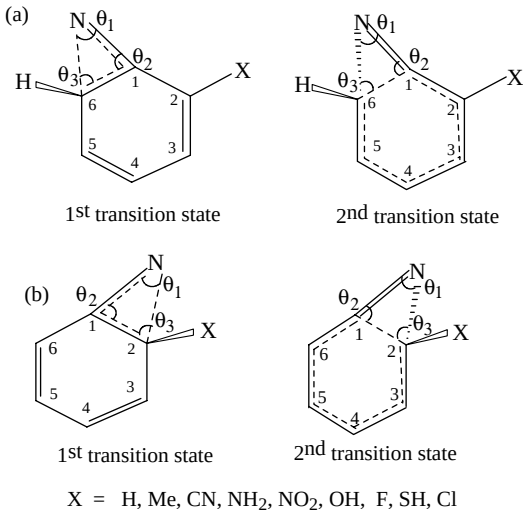


Fig. 2. Geometry parameters for the transition states in ring expansion of *ortho*-substituted phenylnitrenes toward (a) the unsubstituted side, (b) the substituted side.

Both the steps described above thus involve cyclic transition states as seen in Fig. 1. The transition state for the first step centers around a triangular moiety incorporating the nitrogen atom and two adjacent carbon atoms of the phenyl ring. The transition state for the second step centers around a six-membered ring moiety incorporating the breaking C–C single bond and five other C–C bonds, with six electrons delocalised over the six-membered ring. One may note that both the transition states are of a bicyclic type, including a three-membered ring and a six-membered carbocycle.

The net rearrangement reaction can thus lead to two isomeric keteneimine products, where the relative preponderance of one over the other depends primarily on the first step. The factor here is the preferred direction for insertion of the nitrene atom, viz., towards the substituted side or towards the unsubstituted side of the phenyl ring. The activation energy for this first step rather than the reaction enthalpy is reckoned here as the chief determinant of reaction facility owing to the short life of the species involved, since the kinetic aspect is expected to exert a greater deciding influence than the thermodynamic aspect here.

### *1.2. Previous theoretical work*

The two-step ring expansion [6] of singlet phenylnitrene was studied by the CASSCF and CASPT2N methods using 6-31G*, cc-pVDZ and 6-311G basis sets. The initial rearrangement to azepine gave a barrier of 6 kcal/mol, with a smaller barrier of 3 kcal/mol for the subsequent step of rearrangement of azepine to the keteneimine product. Ring expansion [8] of perfluorophenyl- and perfluoro-2-napthylnitrenes to keteimines was studied by the B3LYP/6-31G strategy. Isomerisation of perfluoro-2-napthylnitrene

gave two rearrangement possibilities, where keteneimine formation was favoured over the other by 10 kcal/mol. Triplet arylnitrenes were found to be lower in energy than the keteneimines, so that isomerisation in the triplet state appears unlikely. Ring expansions of fluorinated arylnitrenes [7,9,11,12] were studied at the CASPT2N/cc-pVDZ//CASSCF(8,8)/6-31G* level, which predicted the first step (nitrene insertion) as the rate-determining one. Ring expansion away from the fluorine side was favoured over expansion towards the substituted side by 3 kcal/mol. Fluoro, methyl and chloro groups at the *ortho* position increased barrier heights, suggesting steric and electronic effects.

### 1.3. Scope and aims of study

We choose nine singlet *ortho* substituted phenylnitrenes, numbered **1** to **9** in the tables, with the general formula X–$C_6H_4$–N, where X = H, F, OH, $NH_2$, Cl, SH, Me, CN and $NO_2$ for nitrenes **1** to **9**, respectively. This study aims only for *qualitative* comparisons concerning substituent effects upon kinetic and thermodynamic facility of the two steps of the ring expansion reaction. The multiplicity of cases studied is expected to yield some meaningful qualitative trends here. Comparison of activation energies for the first and second step would help predict which one is the rate-determining step for the ring expansion. From the data generated, predictions are also made as to whether ring expansion is more feasible towards the unsubstituted or the substituted side, predicting the major keteneimine product for each case. We also examine the competition between the ring expansion reaction and the intersystem crossing to the triplet state for each case, comparing the enthalpy for the net ring expansion reaction with the calculated singlet–triplet splitting.

## 2. Theoretical methodology

The semi-empirical AM1 SCF-MO [36] of the MOPAC 6.0 package was used for the 9 singlet phenylnitrenes, 17 azepine intermediates, 17 keteneimine products and 34 transition states. Their geometries were fully optimised by the Davidon–Fletcher–Powell or the Broyden–Fletcher–Goldfarb–Shanno algorithms [37]. The UHF procedure was used to treat the triplet state of the phenylnitrenes. Transition states for both steps of the rearrangement were located by the SADDLE keyword of the MOPAC package, which interpolates between the reactant and the product, locating the transition state by a reverse search strategy. Each transition state structure is confirmed as such by diagonalising the force constant matrix to yield one single negative eigenvalue.

### 2.1. Ring expansion possibilities

Both steps involved in the ring expansion mechanism (nitrene insertion and electrocyclic ring opening) were studied in terms of reaction enthalpies and activation energy barriers. For each case, note was taken of the possibility of ring expansion towards the unsubstituted as well as the substituted side. Reaction enthalpies for ring expansion towards the *unsubstituted* side were labeled as $\Delta H_{us}(1)$ and $\Delta H_{us}(2)$ for the first and second steps respectively, given in Eqs. (1) and (2) below, while the corresponding activation enthalpies were labeled as $E_{us}(1)$ and $E_{us}(2)$ for the first and second steps, respectively.

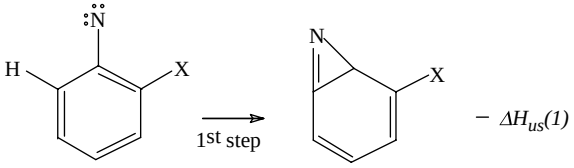


(1)

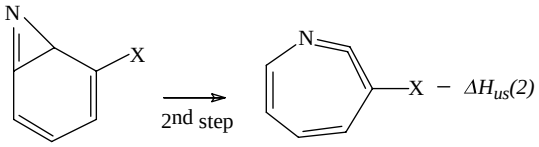


(2)

In similar fashion, ring expansion towards the *substituted* side was studied in terms of the reaction enthalpies $\Delta H_{sb}(1)$ and $\Delta H_{sb}(2)$ and the enthalpies of activation $E_{sb}(1)$ and $E_{sb}(2)$ for the first and second steps respectively, as given below in Eqs. (3) and (4):

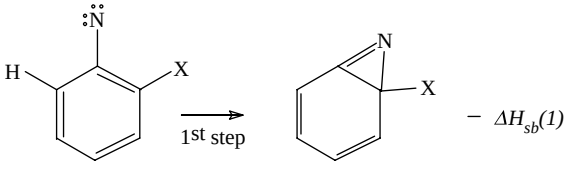


(3)

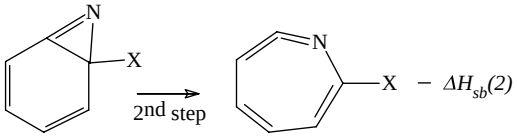


(4)

### 2.2. Transition state geometries

Each ring expansion option incorporates two transition states, where the first pertains to the nitrene insertion step, and the second to the electrocyclic ring opening step. With the possibility for expansion towards the substituted and the unsubstituted side, a total of four transition states arise for each case. Geometry parameters for describing these transition state structures are shown in Fig. 2(a) and (b) for the first and second transition states during ring expansion towards the unsubstituted and the substituted sides respectively.

*2.2.1. First transition state*

For expansion towards the unsubstituted side, focus was laid on the triangular moiety comprising three atoms, labelled as N, C1 and C6. The corresponding triangular moiety for expansion toward the substituted side is described by the three atoms N, C1 and C2. This triangle constitutes the center of the reaction for the first step. The geometrical parameters for the first transition state during expansion towards the *unsubstituted* side are depicted in Fig. 2(a) and include the bond distances $R_{nc1}$, $R_{nc6}$ and $R_{cc}$ for the N–C1, N–C6 and C1–C6 bonds, along with the bond angles ($\theta_1$ and $\theta_2$ comprising the atoms C1–N–C6 and N–C1–C2 in turn respectively. Also included are the dihedral angles $\phi_1$ and $\varphi_2$ encompassing the atoms N–C1–C2–C3 and the atoms C2–C1–C6–C5 in turn respectively. For ring expansion towards the *substituted* side as shown in Fig. 2(b), geometry parameters of the triangle moiety include the bond lengths $R_{nc1}$, $R_{nc2}$ and $R_{cc}$ for the N–C1, N–C2 and C1–C2 bonds, the bond angles $\theta_1$ and $\theta_2$ comprising the atoms C1–N–C2 and N–C1–C6 in turn respectively, along with the dihedral angles $\phi_1$ and $\varphi_2$ encompassing the atoms N–C1–C6–C5 and the atoms C6–C1–C2–C3 in turn respectively.

*2.2.2. Second transition state*

The carbocyclic hexagonal moiety at the center of the transition state for the second step may be described as follows. For ring expansion towards the *unsubstituted* side, as given in Fig. 2(a), the geometry parameters include the bond lengths $R_{16}$, $R_{23}$ and $R_{45}$ for the breaking C1–C6 single bond, the C2–C3 double bond and the C4–C5 double bond respectively, the bond angles $\theta_1$ and $\theta_2$ for the C1–N–C6 and N1–C1–C2 angles respectively, and the dihedral angles $\phi_1$ and $\phi_2$ encompassing the N–C1–C2–C3 and the C5–C6–C1–C2 atoms in turn respectively. For ring expansion towards the *substituted* side, as given in Fig. 2(b), the geometry parameters include the bond lengths $R_{12}$, $R_{34}$ and $R_{56}$ for the breaking C1–C2 single bond, the C3–C4 double bond and the C5–C6 double bond respectively, the bond angles $\theta_1$ and $\theta_2$ for the C1–N–C2 and N1–C1–C6 angles respectively, and the dihedral angles $\phi_1$ and $\phi_2$ which encompass the atoms N–C1–C6–C5 and the atoms C6–C1–C2–C3 in turn respectively. Note that the triangular moiety existing in the second transition state is not described in detail since it does not constitute the actual center of the electrocyclic ring opening reaction.

For both directions of ring expansion, the $\phi_1$ dihedral describes the orientation of the triangular N–C–C moiety with respect to the carbocyclic hexagonal moiety, while the $\phi_2$ dihedral helps to describes the planarity of this six-membered ring moiety.

*2.3. Competition with decay to triplet phenylnitrene*

The scope for competition between the ring expansion reaction in the singlet phenylnitrene and its decay to the triplet state may be gauged by comparing the overall energetics of the ring expansion reaction with the singlet–triplet splitting $\Delta\Delta H_{st}$ for each phenylnitrene species. The highest point along the ring expansion pathway would correspond to the energy of the higher energy transition state (out of the two involved) relative to the starting phenylnitrene reactant. The overall thermodynamic facility of ring expansion may be given by the enthalpy $\Delta H_R$ for the net rearrangement (phenylnitrene to keteneimine). These enthalpy quantities may be compared with the calculated singlet–triplet splittings of each phenylnitrene to estimate the extent of competition between the two processes. From the purely thermodynamic point of view, the relative degree of this competition may be expressed as the enthalpy term $\Delta\Delta E_{rt}$, which is the energy difference between the singlet–triplet splitting $\Delta\Delta H_{st}$ and the net ring expansion enthalpy $\Delta H_R$(us) or $\Delta H_R$(sb) for expansion towards the unsubsituted and substituted sides respectively, depending on which is more favourable energetically.

## 3. Results and discussions

The AM1 results are discussed with respect to (i) kinetic and thermodynamic criteria for reaction facility, (ii) geometry characteristics of the transition states, and (iii) competition between ring expansion and decay to the triplet state of the nitrene, as given below.

*3.1. Kinetic and thermodynamic criteria for ring expansion*

Tables 1 and 2 shows the AM1 data for ring expansion of singlet phenylnitrenes, firstly towards the unsubstituted side of the ring (Table 1) and then towards the substituted side of the ring (Table 2). Kinetic and thermodynamic facilities for ring expansion are respectively indicated by the AM1 activation energy $E_{us}$ and the reaction enthalpy $\Delta H_{us}$, which are studied in the context of the effects of the *ortho* substituent *X* for each case. These two criteria are then further discussed below (Section 3.4) to predict the favoured direction for ring expansion in each case. The activation barriers for the two successive steps of the ring expansion are also compared to predict which step would be the rate-determining one.

*3.2. Expansion toward unsubstituted side*

Table 1 presents the AM1 data for the two steps of the ring expansion reaction for the nine substituted phenylnitrenes, with direction of ring expansion towards the *unsubstituted* side of the phenyl ring as given in Fig. 1(a). This is indicated by attaching **a** to the number of the nitrene entered into the table, e.g. **2a** for *o*-fluorophenylnitrene. The first step (yielding the azepine intermediate) is described by the activation energy $E_{us}(1)$ and the reaction enthalpy $\Delta H_{us}(1)$. The second step (electrocyclic ring opening of

Table 1
AM1 data[a] for the ring expansion of *o*-substituted phenylnitrenes to keteneimines by two-step migration of bonds (where the 1st and the 2nd stages pertain to the two successive steps of the rearrangement reaction, respectively); here, the initial bond migration is towards the unsubstituted side of the phenyl ring (Fig. 1)

| No | System | 1st Step | | | 2nd Step | | |
|---|---|---|---|---|---|---|---|
| | | $\Delta H_{us}(1)$ | $E_{us}(1)$ | $\nu_i$ | $\Delta H_{us}(2)$ | $E_{us}(2)$ | $\nu_i$ |
| **1** | H–$C_6H_4$–N | −3.37 | 16.15 | −0.059 | −19.05 | 9.42 | −2.218 |
| **2a** | F–$C_6H_4$–N | 1.41 | 19.58 | −0.840 | −18.48 | 11.27 | −2.237 |
| **3a** | OH–$C_6H_4$–N | 9.15 | 26.15 | −1.025 | −20.16 | 11.37 | −2.221 |
| **4a** | $NH_2$–$C_6H_4$–N | 11.47 | 28.14 | −1.146 | −19.48 | 12.27 | −2.405 |
| **5a** | Cl–$C_6H_4$–N | −2.11 | 16.63 | −0.687 | −19.10 | 10.17 | −2.218 |
| **6a** | SH–$C_6H_4$–N | 2.20 | 20.53 | −0.907 | −20.86 | 9.92 | −2.249 |
| **7a** | Me–$C_6H_4$–N | −3.05 | 16.58 | −0.795 | −18.86 | 10.52 | −2.191 |
| **8a** | CN–$C_6H_4$–N | −4.89 | 14.75 | −0.661 | −19.52 | 10.27 | −2.172 |
| **9a** | $NO_2$–$C_6H_4$–N | −5.73 | 14.20 | −0.815 | −19.40 | 8.89 | −2.043 |

[a] Enthalpy terms in kcal/mol; $\nu_i$ in millidyne/Å.

azepine to give keteneimene) is described by the activation energy $E_{us}(2)$ and the reaction enthalpy $\Delta H_{us}(2)$.

Reaction enthalpies $\Delta H_{us}(1)$ for the first step are usually small (−5.73–11.47 kcal/mol), suggesting the bicyclic azepine intermediate is generally somewhat less stable than the parent phenylnitrene itself, even though a new sigma N–C bond is formed. Sophisticated calculations at the CASPT2N//CASSCF(8,8)/6-31G* level [6] predict reaction enthalpies of 4.7 kcal/mol for the unsubstituted case and 6.1 kcal/mol for the *o*-fluoronitrene case, showing that the AM1 values are on the high side. The unstable nature of the azepine arises probably from the strain present in the unsaturated three-membered azirine ring moiety. Activation energies $E_{us}(1)$ for the first step are quite large (between 14.20 and 28.14 kcal/mol), indicating that nitrene insertion is not very favourable kinetically. This is quite understandable considering the significant bond re-structuring that accompanies the first step of the ring expansion reaction, besides the presence of the newly-forming strained three-membered ring in the transition state itself. These values may be compared with the CASPT2N//CASSCF(8,8)/6-31G* values of 8.9 kcal/mol for unsubstituted phenylnitrene and 9.5 kcal/mol for *o*-fluoronitrene [6]. Thus, both the AM1 and the sophisticated levels of calculation predict that fluorine substitution disfavours the first step of ring expansion.

The second step of ring expansion (azepine to ketenimine) gives negative values (−18.48 to −20.86 kcal/mol) for the reaction enthalpy $\Delta H_{us}(2)$. This points to the greater thermodynamic stability of the keteimine compared to the azepine intermediate, attributable chiefly to release from the constraints of ring strain in the former. The activation energies $E_{us}(2)$ for this second step (8.89–12.27 kcal/mol) are in each case lower than those for the first step, implying greater kinetic facility for the former. The *first step* is thus predicted to be the rate-determining step for the ring expansion reaction here, which is also predicted by CASSCF and CASPT2N calculations on unsubstituted phenylnitrene [6].

### 3.2.1. Substituent effects

The presence of different *ortho* substituents *X* (*X*=F, OH, $NH_2$, Cl, SH, Me, CN and $NO_2$) creates differences in kinetic and thermodynamic facilities for the two steps of the ring expansion. The reaction enthalpy $\Delta H_{us}(1)$ for the first step gives the order for thermodynamic facility with respect to the substituent *X* as $NO_2$ > CN > H > Me > Cl > F > SH > OH > $NH_2$. This order suggests electron withdrawal as

Table 2
AM1 data[a] for the ring expansion of *o*-substituted phenylnitrenes to keteneimines by two-step migration of bonds (where the 1st and the 2nd stages pertain to the two successive steps of the rearrangement reaction respectively); here, the initial bond migration is towards the substituted side of the phenyl ring (Fig. 1)

| No | System | 1st Step | | | 2nd Step | | |
|---|---|---|---|---|---|---|---|
| | | $\Delta H_{sb}(1)$ | $E_{sb}(1)$ | $\nu_i$ | $\Delta H_{sb}(2)$ | $E_{sb}(2)$ | $\nu_i$ |
| **1** | H–$C_6H_4$–N | −3.37 | 16.15 | −0.059 | −19.05 | 9.42 | −2.218 |
| **2b** | F–$C_6H_4$–N | 4.13 | 20.96 | −0.873 | −21.12 | 7.40 | −2.011 |
| **3b** | OH–$C_6H_4$–N | 10.69 | 26.93 | −1.173 | −22.97 | 5.97 | −1.827 |
| **4b** | $NH_2$–$C_6H_4$–N | 16.00 | 26.46 | −1.069 | −23.31 | 12.27 | −1.621 |
| **5b** | Cl–$C_6H_4$–N | −2.34 | 19.27 | −0.857 | −19.54 | 8.50 | −2.149 |
| **6b** | SH–$C_6H_4$–N | 4.58 | 24.17 | −1.074 | −23.13 | 5.65 | −1.726 |
| **7b** | Me–$C_6H_4$–N | −0.54 | 18.53 | −0.761 | −20.85 | 8.28 | −2.027 |
| **8b** | CN–$C_6H_4$–N | −3.38 | 15.85 | −0.695 | −18.64 | 8.74 | −1.892 |
| **9b** | $NO_2$–$C_6H_4$–N | −7.41 | 15.79 | −0.752 | −15.65 | 8.91 | −1.800 |

[a] Enthalpy terms in kcal/mol; $\nu_i$ in millidyne/Å.

well as electronegativity effects involving the substituent *X*. Electron-withdrawing substituents ($NO_2$ and CN) promote this rearrangement step, while electronegative substituents (like OH and $NH_2$) defacilitate it from the thermodynamic point of view. Electron-withdrawing groups stabilise the bicyclic azepine intermediate and vice versa for the electronegative groups. These substituent effects arise since the substituent group *X* is in conjugation with the moving electron pair for this step, being *ortho* to the nitrene nitrogen.

Similar substituent effects operate on the activation energy $E_{us}(1)$ for the first step, where the order of decreasing kinetic facility for this step with respect to the substituent *X* takes the form $NO_2 > CN > H > Me > Cl > F > SH > OH > NH_2$, exactly the same as that above for thermodynamic facility of this step. Kinetic facility for nitrene insertion is augmented by electron-withdrawing substituents and vice versa for the electron-donating substituents. Both thermodynamic and kinetic criteria coincide in predicting the order for relative facility with respect to substituent *X* as $NO_2 > CN > H > Me > Cl > F > SH > OH > NH_2$. This arises from resonance effects of the *ortho* substituent X upon stability of the intermediate azepine as well as of the transition state itself.

Substituent effects upon the reaction enthalpy $\Delta H_{us}(2)$ for the second step (azepine collapse to ketenimine) are small compared to the first step, since the range of values is narrower (−20.86 to −19.05 kcal/mol), indicating that the presence of different substituents does not have that much effect on the relative stability of the ketenimine. The activation energy $E_{us}(2)$ for the second step also has a narrower range (8.89–12.27 kcal/mol) than the first step. The order for thermodynamic facility of the second step with respect to substituent *X* given by the $\Delta H_{us}(2)$ index is $SH > OH > CN \approx NH_2 \approx NO_2 > Cl > H > Me > F$. The order for kinetic facility given by the $E_{us}(2)$ index is $NO_2 > H > SH > Cl > CN > Me > F > OH > NH_2$. The two orderings are quite different and interpretation is difficult.

### 3.3. Expansion toward substituted side

Table 2 gives the AM1 data for ring expansion toward the *substituted* side of the aromatic ring by two-step migration. This is indicated by attaching **b** to the number of the nitrene entered into the table. The activation energy $E_{sb}(1)$ for the first step of ring expansion (nitrene to azepine) ranges from 15.79 to 26.93 kcal/mol, which for each case is larger than the activation energy $E_{sb}(2)$ for the second step (azepine to keteneimine) which ranges from 5.65 to 12.29 kcal/mol. This is the same as the trend obtained for ring expansion towards the unsubstituted side, and again indicates the greater kinetic instability of the bicyclic intermediate compared to the phenylnitrene reactant. The reaction enthalpy $\Delta H_{sb}(1)$ for the first step ranges from −7.41 to 16.00 kcal/mol, in every case indicating less thermodynamic facility for the first step compared to the second step (associated with an enthalpy index $\Delta H_{sb}(2)$ range from −23.31 to −15.65 kcal/mol). Thus, for all cases of phenylnitrene ring expansion here, whether towards the unsubstituted side or towards the substituted side, the second step is kinetically and thermodynamically more favourable than the first step (the rate-limiting one).

#### 3.3.1. Substituent effects

AM1 data for the effect of substituents on ring expansion toward the substituted side of the ring are presented in Table 2. Kinetic facility for the first step, as given by the $E_{sb}(1)$ index, follows the order: $NO_2 > CN > H > Me > Cl > F > SH > NH_2 > OH$. Thermodynamic facility for this step, as given by $\Delta H_{sb}(1)$, follows a similar order, viz., $NO_2 > CN \approx H > Me > Cl > F > SH > OH > NH_2$. This order is the same as that given by the reaction enthalpy and activation energy for the first step of expansion towards the unsubstituted side as given above. It thus emerges that both thermodynamic and kinetic facilities of the first step of ring expansion are promoted by electron-withdrawing substituents *X* at the *ortho* position of the ring, and vice versa. This is regardless of the direction of nitrene insertion, whether towards the substituted or towards the unsubstituted side. Substituent effects operate in this fashion due to the effect of the *ortho* substituted group upon the moving electron pair during nitrene insertion, where the substituent X is in conjugation with the moving electrion pair.

For the second step of ring expansion towards the substituted side, the enthalpy index $\Delta H_{sb}(2)$ ranges from −23.31 to −15.65 kcal/mol, while the activation energy $E_{sb}(2)$ ranges from 5.65 to 12.27 kcal/mol. Here again, thermodynamic and kinetic facility of the second step is greater than for the first step. Thermodynamic facility for the second step follows the order $NH_2 > SH > OH > F > Me > H > CN > NO_2$. Kinetic facility, as given by $E_{sb}(2)$, gives a different order, viz., $SH > OH > F > Me > Cl > CN > NO_2 > H > NH_2$.

The *first* step of nitrene insertion is thus predicted to be rate-determining for ring expansion towards both substituted and unsubstituted sides. Similar effects of the *ortho* substituent *X* operate for both options, where electron-withdrawing substituents favour the reaction thermodynamically and kinetically, being in conjugation with the incoming electron pair from the nitrene atom, and promotes its moving away from the nitrene atom.

These AM1 reaction enthalpies and activation barriers are somewhat large in value compared to the values earlier obtained for similar quantities in arylnitrene ring expansions through use of the CASSCF and CASPT2N methods with 6-31G*, cc-pVDZ and 6-311G basis sets [7] and also at the CASPT2N//CASSCF(8,8)/6-31G* level. The value of these AM1 calculations here lies in the relatively large number of different systems studied, so that the effects of various substituent groups on ring expansion facility may be, at least qualitatively speaking, fairly reliably discerned.

That the AM1 method can yield results regarding activation barriers which are in qualitative agreement with more accurate methods has been shown by us [38] for 1,2 hydrogen shifts in carbene rearrangements to alkene products.

### 3.4. Preferred direction of ring expansion

One now uses the above results to help predict the direction in which the ring expansion is favoured—whether towards the unsubstituted side or towards the substituted side for each of the 8 *ortho*-substituted phenylnitrenes **35**–**42**. The main factor which controls the direction of ring expansion is the relative kinetic facility of the reaction. The short lives of the reactant and the intermediates invoke the kinetic factor (given by the activation energy $E_{us}$ and $E_{sb}$) rather than the thermodynamic factor (given by the reaction enthalpy $\Delta H_{us}$ and $\Delta H_{sb}$). Here, the *first step* of the reaction (nitrene insertion and azepine formation) is the crucial one, being the rate-determining step as established earlier. The strategy here thus involves comparison of magnitude of the activation enthalpies $E_{us}(1)$and $E_{sb}(1)$ for the first step of ring expansion towards the unsubstituted and substituted sides as per the values given in Tables 1 and 2.

The relative magnitudes of the activation energy $E_{sb}(1)$ indicate that the presence of *ortho*-substituents like F, OH, Cl, SH, Me, CN and $NO_2$ in the phenylnitrene favours nitrene insertion toward the *unsubstituted* side to a greater or lesser degree. However, when the $NH_2$ group is present, the direction of insertion of the nitrene atom is more favourable towards the substituted side. Apparently, the main factor introduced by the presence of substituent at the *ortho* position is one of *steric hindrance* during insertion. This effect is also shown by comparing activation energies between the substituted and unsubstituted sides for cases having atoms of the same periodic table group. The activation energies are larger for cases having the second row elements (S and Cl) than those having the first row elements (O and F), which is apparently largely a steric factor. The role of electron-donation from the lone pairs of the heteroatom substituent is also a factor, which is, however, largely overridden by the steric factor except for the case of the strongly electron-donating $NH_2$ group.

The second step of the reaction is not very important for determining the direction of ring expansion since it is the first step which is rate-determining as mentioned earlier. One notes, however, that for the second step, the enthalpy of activation $E_{sb}(2)$ for ring expansion toward the substituted side is usually larger than that toward the unsubstituted side. This indicates that the presence of the substituent on the bicyclic ring generally favours ring expansion towards the substituted side as compared with the unsubstituted side, here again attributable primarily to a steric effect.

### 3.5. Transition state geometries

Fig. 2(a) and (b) depict the geometries of the transition states for the two steps of the ring expansion of substituted phenylnitrenes toward the unsubstituted and the substituted sides respectively which are shown in Fig. 1(a) and (b) respectively. Tables 3–6 present the AM1 values for selected geometry parameters for the transition states pertaining to both the first and the second steps.

One proposes that the transition state for the *first step* of azepine formation occurs somewhat midway along the reaction pathway between reactant (phenylnitrene) and product (azepine), since the reaction enthalpies $\Delta H_r(1)$ are either small negative or positive (except the amino substituted case **4**). It may be thus expected to display some geometrical characteristics of both the reactant and the product. The *second* transition state (for azepine collapse) is, however, definitely on the 'early' side for all cases, with reaction enthalpies $\Delta H_r(2)$ all negative and of appreciable magnitude. This means that the second transition state would tend to resemble the azepine reactant more than the ketenimine product.

### 3.6. Transition state geometries for expansion towards unsubstituted side

The geometry parameters for the *first* transition state include the bond distances $R_{nc1}$, $R_{nc6}$ and $R_{cc}$, the bond angles $\theta_1$ and $\theta_2$ along with the dihedral angles $\phi_1$ and $\varphi_2$

Table 3
AM1 geometry parameters[a] for the transition state *TS1* involved in the first step (formation of bicyclic azepine intermediate from the phenylnitrene), where bond migration is towards the *unsubstituted* side of the phenyl ring (geometry *para*-meters as described in the text)

| No | Group | $R_{nc1}$ | $R_{nc2}$ | $R_{cc}$ | $\theta_1$ | $\theta_2$ | $\phi_1$ | $\phi_2$ |
|---|---|---|---|---|---|---|---|---|
| **1** | H–$C_6H_4$ | 1.275 | 1.987 | 1.454 | 46.92 | 140.27 | 124.34 | 30.04 |
| **2a** | F–$C_6H_4$ | 1.271 | 1.943 | 1.453 | 48.37 | 140.69 | 120.48 | 28.92 |
| **3a** | OH–$C_6H_4$ | 1.270 | 1.920 | 1.452 | 49.16 | 141.06 | 115.14 | 31.06 |
| **4a** | $NH_2$–$C_6H_4$ | 1.268 | 1.922 | 1.453 | 49.12 | 140.55 | 111.59 | 34.50 |
| **5a** | Cl–$C_6H_4$ | 1.273 | 1.973 | 1.453 | 47.36 | 140.31 | 122.97 | 30.02 |
| **6a** | SH–$C_6H_4$ | 1.271 | 1.937 | 1.454 | 48.65 | 140.85 | 120.01 | 30.70 |
| **7a** | Me–$C_6H_4$ | 1.273 | 1.940 | 1.450 | 48.39 | 140.47 | 123.30 | 28.33 |
| **8a** | CN–$C_6H_4$ | 1.275 | 1.958 | 1.453 | 47.90 | 140.26 | 125.57 | 26.94 |
| **9a** | $NO_2$–$C_6H_4$ | 1.268 | 1.896 | 1.448 | 49.76 | 143.23 | 123.32 | 26.89 |

[a] Bond lengths in angstrom; bond angles and dihedral angles in degrees.

Table 4
AM1 geometry parameters[a] for the transition state *TS2* involved in the second step (electrocyclic ring opening of the azepine intermediate) to give the ketene–imine product, where initial bond migration is towards the *unsubstituted* side of the phenyl ring (geometry parameters as given in the text)

| No | Group | $R_{23}$ | $R_{45}$ | $R_{16}$ | $\theta_1$ | $\theta_2$ | $\phi_1$ | $?\phi_2$ |
|---|---|---|---|---|---|---|---|---|
| **1** | H–$C_6H_4$ | 1.386 | 1.393 | 1.791 | 81.85 | 159.22 | 38.78 | 30.09 |
| **2a** | F–$C_6H_4$ | 1.400 | 1.382 | 1.776 | 80.87 | 156.96 | 49.49 | 25.62 |
| **3a** | OH–$C_6H_4$ | 1.390 | 1.383 | 1.787 | 81.78 | 158.17 | 42.43 | 28.07 |
| **4a** | $NH_2$–$C_6H_4$ | 1.410 | 1.384 | 1.799 | 82.41 | 159.08 | 43.48 | 28.31 |
| **5a** | Cl–$C_6H_4$ | 1.396 | 1.386 | 1.784 | 81.37 | 158.97 | 42.13 | 29.20 |
| **6a** | SH–$C_6H_4$ | 1.403 | 1.388 | 1.810 | 82.92 | 160.50 | 37.27 | 30.31 |
| **7a** | Me–$C_6H_4$ | 1.394 | 1.385 | 1.788 | 81.64 | 159.76 | 43.63 | 29.96 |
| **8a** | CN–$C_6H_4$ | 1.398 | 1.387 | 1.779 | 81.11 | 158.20 | 47.98 | 27.45 |
| **9a** | $NO_2$–$C_6H_4$ | 1.404 | 1.390 | 1.774 | 80.73 | 159.56 | 44.95 | 29.55 |

[a] Bond lengths in angstrom; bond angles and dihedral angles in degrees.

defined earlier, whose values are presented in Table 3 for the nine cases studied. Within the triangular moiety, the bond distances $R_{nc1}$ (1.268–1.275 Å) for the N–C1 bond are much shorter than the bond distances $R_{nc6}$ (1.896–1.987 Å) for the newly forming N–C6 bond. This is quite understandable in the context of the partial double-bond character of the N–C1 bond and the less than single-bond character of the newly forming N–C6 bond in the transition state. The C1–C6 bond lengths $R_{cc}$ range from 1.448 to 1.454 Å for all cases, lying between a single and double C–C bond in length (with some preponderance towards the latter), and not varying much from case to case. Use of a different Kekule structure for the benzene ring in Fig. 1(a) would in fact suggest that this C1–C6 bond does not take part significantly in the first step of azepine formation, hence its single bond character.

The triangular moiety of the transition state for the first step here resembles a right-angled triangle (the N–C1–C6 angle ranges from 88.30 to 93.25°—data not given). The C1–N–C6 bond angle $\theta_1$ is markedly acute, ranging from 46.92 to 49.76°, indicating that the strained three-membered ring is in the process of formation. The N–C1–C2 angle $\theta_2$ is of interest here since this angle is about 120° in the nitrene reactant, but would increase appreciably in the bicyclic azepine product; in the transition state it ranges from 140.26 to 141.06°, quite a narrow range. The dihedral $\phi_1$ ranges between 111.59 and 125.57°, indicating that the forming triangular moiety is already somewhat out of the plane of the benzene ring. The dihedral $\varphi_2$ ranges from 26.89 to 34.50°, which indicates that the benzene ring is not quite planar in the transition state. There is still, however, some significant delocalisation of the pi electrons for five contiguous C–C bonds, where the C1–C6 bond alone is a little longer than the rest with a lesser degree of pi electron delocalisation present in it.

The geometry parameters describing the *second* transition state are given in Table 4. Here, the N–C1 and N–C6 bond lengths (data not given) closely approach the standard (static) lengths for N=C double bonds and N–C single bonds, showing that these bonds scarcely participate in the second step of ring expansion to ketenimine. The real centre for the reaction corresponding to the second step of ring expansion is actually the hexagonal ring moiety C1–C2–C3–C4–C5–C6 which constituted the benzene ring in the original phenylnitrene reactant. The bond lengths $R_{16}$ for the breaking C1–C6 bond are appreciably longer than for normal C–C single bonds, ranging from 1.774 to 1.810 Å, indicating this bond is in a state of fission. The C2–C3 and C4–C5 bond lengths (ranging from 1.382 to 1.410 Å) are in between single and double C–C bond lengths, pointing to the state of delocalisation of the pi bonds in the transition state. This is not so in the azepine reactant nor in the keteimine product, which both have alternating long and short C–C bond lengths in their ring moieties. One may thus propose that the transition state for the second step is, in

Table 5
AM1 geometry parameters[a] for the transition state *TS1* involved in the first step (formation of bicyclic azepine intermediate from the phenylnitrene), where bond migration is towards the *substituted* side of the phenyl ring (geometry parameters as described in the text)

| No | Group | $R_{nc1}$ | $R_{nc2}$ | $R_{cc}$ | $\theta_1$ | $\theta_2$ | $\phi_1$ | $\phi_2$ |
|---|---|---|---|---|---|---|---|---|
| **1** | H–$C_6H_4$ | 1.275 | 1.987 | 1.454 | 46.92 | 140.27 | 124.34 | 30.04 |
| **2b** | F–$C_6H_4$ | 1.268 | 1.979 | 1.472 | 48.01 | 140.53 | 114.87 | 36.88 |
| **3b** | OH–$C_6H_4$ | 1.271 | 1.909 | 1.460 | 49.86 | 140.65 | 109.42 | 33.55 |
| **4b** | $NH_2$–$C_6H_4$ | 1.260 | 1.902 | 1.487 | 51.34 | 144.34 | 106.51 | 43.08 |
| **5b** | Cl–$C_6H_4$ | 1.274 | 1.962 | 1.463 | 48.18 | 140.20 | 119.42 | 31.44 |
| **6b** | SH–$C_6H_4$ | 1.269 | 1.908 | 1.454 | 49.63 | 141.84 | 118.57 | 31.18 |
| **7b** | Me–$C_6H_4$ | 1.270 | 1.944 | 1.462 | 48.77 | 139.93 | 118.12 | 30.66 |
| **8b** | CN–$C_6H_4$ | 1.275 | 1.941 | 1.469 | 49.18 | 141.06 | 119.61 | 28.43 |
| **9b** | $NO_2$–$C_6H_4$ | 1.277 | 1.963 | 1.469 | 48.42 | 139.69 | 118.52 | 27.70 |

[a] Bond lengths in angstrom; bond angles and dihedral angles in degrees.

Table 6
AM1 geometry parameters[a] for the transition state *TS2* involved in the second step (electrocyclic ring opening of the azepine intermediate) giving the keteneimine product, where initial bond migration is towards the *substituted* side of the phenyl ring (geometry parameters as described in the text)

| No | Group | $R_{34}$ | $R_{56}$ | $R_{12}$ | $\theta_1$ | $\theta_2$ | $\phi_1$ | $\phi_2$ |
|---|---|---|---|---|---|---|---|---|
| **1** | H–$C_6H_4$ | 1.386 | 1.393 | 1.791 | 81.85 | 159.22 | 38.78 | 30.09 |
| **2b** | F–$C_6H_4$ | 1.377 | 1.389 | 1.758 | 79.23 | 158.85 | 48.17 | 30.41 |
| **3b** | OH–$C_6H_4$ | 1.377 | 1.388 | 1.762 | 79.61 | 159.40 | 46.66 | 30.14 |
| **4b** | $NH_2$–$C_6H_4$ | 1.372 | 1.384 | 1.758 | 78.66 | 157.75 | 48.12 | 33.32 |
| **5b** | Cl–$C_6H_4$ | 1.382 | 1.390 | 1.781 | 81.05 | 159.90 | 40.92 | 31.44 |
| **6b** | SH–$C_6H_4$ | 1.374 | 1.382 | 1.746 | 79.00 | 159.74 | 47.26 | 33.01 |
| **7b** | Me–$C_6H_4$ | 1.382 | 1.388 | 1.785 | 81.09 | 159.12 | 41.62 | 32.41 |
| **8b** | CN–$C_6H_4$ | 1.380 | 1.387 | 1.781 | 80.69 | 159.81 | 40.68 | 32.28 |
| **9b** | $NO_2$–$C_6H_4$ | 1.384 | 1.394 | 1.798 | 81.67 | 159.84 | 36.05 | 32.15 |

[a] Bond lengths in angstrom; bond angles and dihedral angles in degrees.

principle, aromatic, although neither reactant nor product here is aromatic.

The C1–N–C6 bond angle $\theta_1$ in the second transition state is of interest here since it is only about 60° in the azepine reactant, but becomes about 120° in the keteimine product. In the transition state, it has an intermediate value range, ranging from 80.87 to 82.92°. The N–C1–C2 angle $\theta_2$ may be expected to be large, since it would become almost 180° in the keteimine product due to the sp hybridised C1 atom present. In the transition state, it ranges from 156.96 to 160.50°. The dihedral $\varphi_1$ ranges from 38.78 to 47.98°, which indicates that the N–C1–C6 triangular moiety is not in the general plane of the carbocyclic ring. The dihedral $\varphi_2$ ranges from 25.62 to 30.09°, which points to the somewhat non-planar shape of the six-membered carbocylic ring itself.

### *3.7. Transition state geometries for expansion towards substituted side*

Tables 5 and 6 present the geometry data for the first and second transition states for ring expansion towards the substituted side of the phenyl ring as portrayed in Fig. 1(b). By and large, these geometry parameters resemble in value those for the cases of expansion towards the unsubstituted side as given earlier in Tables 3 and 4 for the first and the second step processes respectively.

The data of Table 5 for the first transition state gives the value ranges of the bond distances $R_{nc1}$, $R_{nc2}$ and $R_{cc}$ as 1.260–1.277 Å, 1.902–1.987 Å and 1.454–1.487 Å respectively. This data is largely similar to the corresponding data for the case of expansion towards the unsubstituted side as described earlier, and leads to similar conclusions. The bond angle $\theta_1$ ranges here from 46.92 to 51.34°, being quite acute as in the first transition state for expansion towards the unsubstituted side. The N–C1–C2 triangular moiety here is again more-or-less right angled in shape. The bond angle $\theta_1$ here has a range of values similar to the previous case of expansion towards the unsubstituted side. The value range for the dihedral angle $\phi_1$ (139.69–144.34°) indicates here again that the triangular moiety is somewhat out of the plane of the benzene ring. The dihedral $\varphi_2$ ranges from 28.43 to 43.08°, indicating again that the carbocycle is not quite planar.

The geometry data for the second transition state as given in Table 6 corresponds closely to the geometry data of Table 4 (for expansion towards the unsubstituted side). The bond distance $R_{12}$ ranges from 1.746 to 1.798 Å, indicating that the C1–C2 bond is in a state of being broken. The range of values for the C3–C4 and C5–C6 bond lengths indicate partial double bond character for these bonds, from which one may infer the aromatic character of this transition state. The angle $\theta_1$ ranges from 44.37 to 45.36° respectively, again pointing to a scalene triangular shape. The angle $\theta_1$ has

Table 7
Energetics[a] of ring expansion possibilities in substituted phenylnitrenes compared with the singlet–triplet splittings for nine *ortho*-substituted phenylnitrenes

| No | System | $E_{us}(1)$ | $\Delta H_R$(us) | $E_{sb}(1)$ | $\Delta H_R$(sb) | $\Delta\Delta H_{st}$ | $\Delta\Delta E_{rt}$ |
|---|---|---|---|---|---|---|---|
| **1** | H–$C_6H_4$–N | 16.15 | −22.42 | 16.15 | −22.42 | 42.72 | 20.30 |
| **2** | F–$C_6H_4$–N | 19.58 | −17.07 | 20.96 | −16.99 | 40.60 | 23.53 |
| **3** | OH–$C_6H_4$–N | 26.15 | −11.06 | 26.93 | −12.28 | 32.11 | 19.83 |
| **4** | $NH_2$–$C_6H_4$ | 28.14 | −8.01 | 26.46 | −7.31 | 29.82 | 21.82 |
| **5** | Cl–$C_6H_4$–N | 16.63 | −21.21 | 19.27 | −21.88 | 42.14 | 20.26 |
| **6** | SH–$C_6H_4$–N | 20.53 | −18.66 | 24.17 | −18.55 | 36.73 | 16.07 |
| **7** | Me–$C_6H_4$–N | 16.58 | −21.91 | 18.53 | −21.39 | 41.99 | 20.08 |
| **8** | CN–$C_6H_4$–N | 14.75 | −24.41 | 15.85 | −22.02 | 44.29 | 19.88 |
| **9** | $NO_2$–$C_6H_4$–N | 14.20 | −25.13 | 15.79 | −23.03 | 44.13 | 19.00 |

[a] All enthalpy terms in kcal/mol.

a range similar to that in the previous case of expansion towards the unsubstituted side. The dihedral angle $\phi_1$ ranges from 36.05 to 48.17°, implying the triangular moiety here is also not in the plane of the carbocyclic ring. This ring itself is not quite planar, as seen from values of the dihedral $\phi_2$ (30.09–33.32°).

### 3.8. Competition with decay to triplet nitrene

Table 7 presents the AM1 values of the activation barriers $E_{us}(1)$ and $E_{sb}(1)$ for the first step of ring expansion towards the unsubstituted and substituted sides respectively, along with the net reaction enthalpies $\Delta H_R$(us) and $\Delta H_R$(sb) for overall rearrangement of the phenylnitrene to the keteneimine from the unsubstituted and substituted siders respectively. For each case, it is the more negative of two net reaction enthalpies $\Delta H_R$(us) and $\Delta H_R$(sb) which is taken into consideration. Also given are the singlet–triplet energy gaps $\Delta\Delta H_{st}$, for the nine different *ortho* substituted phenylnitrene cases studied here, where the values are all positive by the convention that the a triplet ground state is indicated by positive values of the singlet–triplet splitting. The actual energy of inter-system crossing over to the triplet state is the *negative* of this quantity. The energy difference $\Delta\Delta E_{st}$ represents the extent to which decay to the triplet state is favoured over the net ring expansion reaction, and is calculated as given by Eq. (5) below:

$$\Delta\Delta E_s = \Delta\Delta H_{st} + \Delta H_R(\text{us}) \text{ [or } \Delta H_R(\text{sb})] \quad (5)$$

The AM1 data presents the ring expansion possibility as invariably less favourable than the possibility of decay to the triplet state. The rearrangement reaction course involves an activation barrier for every case, while decay to the triplet state does not. The energy difference $\Delta\Delta E_{st}$ favouring decay to the triplet state ranges from 16.07 to 21.82 kcal/mol, predicting that the SH-substituted case **6** would present the most competition from ring expansion, while the least favourable chance for ring expansion is represented by the $NH_2$-substituted case **4**.

## 4. Concluding remarks

This AM1 SCF-MO study of ring expansion in several substituted phenylnitrenes leads to the following conclusions and inferences:

1. The first step of nitrene insertion is the rate determining step in all cases.
2. The bicyclic azepine intermediate produced in the first step of ring expansion is unstable compared to the final ketenimine product.
3. Electron-withdrawing *ortho* substituents in phenylnitrenes favour both the nitrene insertion step and the electrocyclic ring opening step, especially the former, for which the order of reaction facility with respect to the substituent is predicted as $NO_2 > CN > H > Me > Cl > F > SH > OH > NH_2$.
4. Ring expansion towards the unsubstituted side is favoured over expansion towards the substituted side of the ring for all cases (except the amino substituted case) since steric effects generally predominate over electronic effects.
5. The first transition state is more or less midway along the reaction coordinate for the first step, while the second transition state is definitely more on the 'early' side.
6. In both the transition states, the triangular moiety is not co-planar with the carbocyclic ring moiety, though the second transition state has some aromatic character.
7. Competition between ring expansion and decay of the singlet phenylnitrene to the triplet state is generally predicted to proceed in favour of decay to the triplet state.

## References

[1] S.P. McManus, Organic Reactive Intermediates, Academic Press, New York, 1973.
[2] C.J. Moody, G.H. Whitham, Reactive Intermediates, Oxford Science Publications, 1992.
[3] W.D. Crow, C. Wentrup, Tetrahedron Lett. 1968; 6149.
[4] R.C. Joines, A.B. Turner, W.M. Jones, J. Am. Chem. Soc. 91 (1969) 7754.
[5] J.A. Myers, R.C. Joines, W.M. Jones, J. Am. Chem. Soc. 92 (1970) 4740.
[6] W.L. Karney, W.T. Borden, J. Am. Chem. Soc. 119 (1997) 1378.
[7] W.L. Karney, W.T. Borden, J. Am. Chem. Soc. 119 (1997) 3347.
[8] B. Kozankiewicz, I. Deperasinska, H.B. Zhai, Z. Zhu, C.M. Hadad, J. Phys. Chem. A 103 (1999) 5003.
[9] B.A. Smith, C.J. Cramer, J. Am. Chem. Soc. 118 (1996) 5490.
[10] D.D. Shillady, C. Trindle, Theor. Chim. Acta 43 (1976) 137.
[11] K.A. Schnapp, M.S. Platz, Bioconjugate Chem. 4 (1993) 178.
[12] M.S. Platz, Acc. Chem. Res. 28 (1995) 487.
[13] M. Apple, R. Huisgen, Chem. Ber. 92 (1959) 2961.
[14] M. Ogata, H. Kano, H. Matsumuto, Chem. Commun. 1968; 398.
[15] W.von E. Deoring, R.A. Odum, Tetrahedron 22 (1966) 81.
[16] W. Lwowski, F.P. Woerner, J. Am. Chem. Soc. 87 (1965) 5491.
[17] R. Huisgen, M. Appl, Chem. Ber. 91 (1958) 12.
[18] N.P. Gritzan, Z. Zhu, C.M. Hadad, M.S. Platz, J. Am. Chem. Soc. 121 (1999) 1202.
[19] N.P. Gritsan, T. Yuzawa, M.S. Platz, J. Am. Chem. Soc. 119 (1997) 5059.
[20] R. Poe, K. Schnapp, M.J.T. Young, J. Grayzar, M.S. Platz, J. Am. Chem. Soc. 114 (1992) 5054.
[21] A. Marcinek, E. Leyva, D. Whitt, M.S. Platz, J. Am. Chem. Soc. 115 (1993) 8609.
[22] E. Leyva, M.S. Platz, G. Persy, J. Wirz, J. Am. Chem. Soc. 108 (1986) 3783.
[23] C. Wentrup, C. Mayor, R. Gleiter, Helv. Chim. Acta 55 (1972) 2629.
[24] C. Wentrup, C. Thetaz, R. Gleiter, Helv. Chim. Acta 55 (1972) 2633.
[25] M.C. Lopez, N.P. Gritzan, Z. Zhu, M.S. platz, J. Phys. Chem. A 104 (2000) 9681.
[26] A. Marcinek, M.S. Platz, S.Y. Chan, R. Floresca, K. Rajagopalan, M. Golinski, D. Watt, J. Phys. Chem. 98 (1994) 412.
[27] A. Albini, G. Bettinetti, G. Minoli, J. Am. Chem. Soc. 121 (1999) 3104.

[28] N.P. Gritsan, D. Tigelaar, M.S. Platz, J. Phys. Chem. A 103 (1999) 4465.
[29] A. Reiser, V. Frazer, Nature (London) 208 (1965) 682.
[30] A. Reiser, H.M. Wagner, R. Marley, G. Bowes, Trans. Faraday Soc. 63 (1967) 2403.
[31] J.C. Hayes, R.S. Sheridan, J. Am. Chem. Soc. 112 (1990) 5879.
[32] Y.Z. Li, J.P. Kirby, M.W. George, M. Poliakoff, G.B. Schuster, J. Am. Chem. Soc. 110 (1988) 8092.
[33] J. Morawietz, W. Sander, J. Org. Chem. 61 (1996) 4351.
[34] T. de Boer, J.I.G. Cadogan, H.M. McWilliam, A.G. Rowley, J. Chem. Soc., Perkin Trans. 2 1975; 554.
[35] O.L. Chapman, J.P. LeRoux, J. Am. Chem. Soc. 100 (1978) 282.
[36] M.J.S. Dewar, E.C. Zoebisch, E.F. Healy, J.J.P. Stewart, J. Am. Chem. Soc. 107 (1985) 3902.
[37] J.J.P. Stewart, Quantum Chem. Prog. Exch. Bull. 3 (1983) 43.
[38] P.G.S. Dkhar, R.H.D. Lyngdoh, Indian J. Chem. Sect. B, (in press).